Non-thermal X-ray emission from Anomalous X-ray Pulsars

den Hartog, P.R.

Chapter 1

Introduction

In August 2007 in a hotel in Montréal, I entered the breakfast room where I saw two people – a man and a woman – having breakfast together. The woman – early sixties – had dark hair which was tending to turn grey and she wore a long dress printed with flowers. The man – who was quite a bit older, early eighties – had white-grey hair and he wore a light-coloured suit. I recognized the couple. In fact, the reason for me and about 150 other scientists visiting Montréal was because of the discovery they made 40 years before (August 1967). These people were *Jocelyn Bell Burnell* and *Antony Hewish*, the discoverers of a new kind of astronomical objects: **pulsars** (Hewish et al. 1968). With their discovery a new field of astronomy was born. Even after 40 years of research there are still a lot of gaps in our knowledge of pulsars. Even to date exciting and surprising discoveries are still being made on a regular basis. Pulsar science is even after 40 years flourishing and as exciting as ever.

1.1 A historical introduction

Most discoveries are made by coincidence. This was also the case with the discovery of pulsars. Jocelyn Bell was a PhD student at the University of Cambridge (under the supervision of Hewish) searching for interstellar scintillation in quasars using the Mullard Radio Astronomy Observatory. In a time with hardly any computers this search meant going over kilometers of paper – on which the radio signals were plotted – by hand and eye. The fact that this discovery was made is a classic example of wanting to understand everything that is in your data. This is what Jocelyn Bell did in 1967. She recognized a handful of 'different' signals out of the countless other events. She would not give up on those signals until their origin would become clear. Firstly, it was recognized that these signals were of astronomical origin as they reappeared after a sidereal day (23h 56m $4\overset{s}{.}1$) in stead of 24h. Secondly, it was found that the signals showed regular pulses after measuring them with a higher time-resolution readout. However, the origin still remained unclear. The discovery of the first pulsar (PSR B1919+21; Hewish et al. 1968) was originally designated as LGM-1, where LGM is the abbreviation for *Little Green Man*. The thought of having discovered an extraterrestrial civilisation disappeared quickly when more regular radio signals with different frequencies were found from different locations (Pilkington et al. 1968). These signals were made by nature.

There are not many examples in astronomy where the theory was leading the observations. The neutron star existed already for more than thirty years as a theoretical object. In a paper discussing the possible origin of cosmic rays Baade & Zwicky (1934) postulated neutron stars as possible products of supernova explosions (see Sect. 1.2) and they were aware that these could have very small radii and extremely high densities. A remarkable prediction considering that the neutron was discovered only two years before (Chadwick 1932). The first neutron-star model was created by Oppenheimer & Volkoff (1939) in which they considered a core of free neutrons in an ideal gas. It was not until the late fifties and early sixties before the first realistic and detailed neutron-star models appeared (Harrison et al. 1958; Cameron 1959).

In proving that neutron stars exist and that pulsars are indeed neutron stars, the Crab nebula – the remnant of the supernova explosion of 1054 – would play an essential role. Baade (1942) and Minkowski (1942) studied the Crab nebula and concluded that most of the (optical) emission showed a continuous spectrum emitted by the inner part of diffuse nebulosity. They argued that this spectrum is likely produced by free-free and free-bound transitions of electrons in a highly ionized gas. One of two visible stars in the centre of the supernova remnant could be the candidate responsible for exciting the nebula. It was remarkable as it did not show any spectral lines. Minkowski (1942) discusses that the mass of the central star should be around one solar mass and that it should have a small radius. Therefore, its density should be very high. However, he did not realize that a neutron star was a possible explanation.

After the detection of the Crab nebula in radio (Bolton et al. 1949) it was argued by Alfvén & Herlofson (1950) that the continuous spectrum from the nebula was caused by synchrotron radiation which is emitted by relativistic electrons moving through a magnetic field. This theory

which Shklovsky (1954) explored thoroughly, suggested that also the explanation of highly polarized optical continuous radiation (Dombrovsky 1954; Oort & Walraven 1956) pointed toward a synchrotron origin rather than the emission mechanism suggested by Minkowski (1942). Oort & Walraven (1956) calculated that these electrons loose their energy within $\sim$200 years, which meant a source must exist which continuously supplies the nebula with new electrons. They suggested as source for the electrons the same continuous-spectrum star which Minkowski (1942) proposed to be the remnant of the supernova. After the discovery of the Crab nebula in X-rays (see below; Bowyer et al. 1964b), Chiu (1964) suggested that the X-rays could be originating from a neutron star. Woltjer (1964) noted that a neutron star with a high magnetic field might somehow be able to produce relativistic electrons.

Just before the publication of the first pulsar (Hewish et al. 1968) Pacini (1967) published a paper on a possible emission mechanism which could feed the Crab nebula continuously. He proposed a rapidly rotating neutron star with a strong magnetic field emitting dipole radiation. Right after the discovery of the first pulsar Gold (1968) and Pacini (1968) suggested that these pulsars could be rotating neutron stars. Scientists were hard to convince (among them was Hewish) and they were clinging to the more conventional idea that pulsars could be white dwarfs. However, the Crab pulsar was soon discovered with 33 ms pulsations (Staelin & Reifenstein 1968). These pulsations were hard to explain for a white dwarf interpretation and were interpreted as the rotation period of the Crab pulsar. When also the spin down of the Crab pulsar was measured (Richards & Comella 1969) which was predicted by Pacini (1968) and Gold (1968) the picture was complete. Pulsars are rotating neutron stars! Cosmic lighthouses radiating beams of radio emission.

However, this is not the full story ...

In the early sixties X-ray astronomy started to take form. As X-rays are shielded by the Earth's atmosphere measurements have to be taken from space using rocket experiments. Therefore, high-energy astrophysics – excluding very high-energy gamma-ray astronomy – is by tradition a space science. A new era in astronomy started after an *Aerobee* rocket was launched with which the first X-ray source outside our solar system was discovered (Giacconi et al. 1962). The source was Scorpius X-1 (Sco X-1), which was confirmed by independent measurements by Bowyer et al. (1964a). Soon thereafter Bowyer et al. (1964b) discovered X-ray emission from the Crab nebula. By the end of the sixties about 20 X-ray sources were located and it was noticed that most of these objects were concentrated along the Galactic plane (Morrison 1967) and therefore likely of Galactic origin. Shklovsky (1967) proposed that the X-rays from Sco X-1 originated from a hot gas flowing onto a neutron star from a close binary companion. It was already noticed that the orbital motion of such a system could indicate the nature of the compact object (which could also be a black hole Zeldovich & Guseynov 1966). Great advances in understanding compact X-ray sources were achieved after the launch of *Uhuru*, the first astronomical satellite at the end of 1970. Within just over two years of observing *Uhuru* detected and localized 339 X-ray sources (Giacconi et al. 1972; Forman et al. 1978).

Moreover, pulsations were detected from Cen X-3 which was therefore the first discovered X-ray pulsar (Giacconi et al. 1971). Binaries with black holes, neutron stars or white dwarfs were all found, as well as single neutron stars. *Uhuru* opened the X-ray window. Progress in neutron-star and X-ray astrophysics would proceed rapidly from now on.

1.2 Neutron-star formation in a nutshell

Neutron stars (and black holes) are the final products of stellar evolution, i.e. stellar corpses. A neutron star can be formed inside a heavy star at the end of its life while the rest of the star explodes in the form of a supernova explosion. The mass of the dying star (more or less) determines whether the compact object will be a neutron star, or a black hole. Most of the neutron stars originate from heavy stars with masses between $\sim 8\,M_\odot$ and $20\,M_\odot$. At the final stages of the star's life silicon burning will start. Within days a massive iron core is produced. Then, the iron will be destroyed into neutrons by photodisintegration because of the extreme core temperatures. Important processes are:

$$^{56}_{26}\mathrm{Fe}^{26+} + \gamma \rightarrow 13\,^{4}_{2}\mathrm{He}^{2+} + 4n \tag{1.1}$$

$$^{4}_{2}\mathrm{He}^{2+} + \gamma \rightarrow 2p^{+} + 2n. \tag{1.2}$$

Degenerate electrons – which are responsible for the pressure inside the core (Pauli exclusion principle) – are captured by protons and therefore the electron-degeneracy pressure in the core is lifted and the core will collapse;

$$p^{+} + e^{-} \rightarrow n + \nu_e \tag{1.3}$$

The hot core cools rapidly by neutrino (ν_e) emission . The core will divide in an inner core and an outer core. Where the infall speed equals the local sound speed the outer core cannot keep up with the inner core. The inner core is formed until the Pauli exclusion principle (neutron degeneracy) prevents further collapse. At that point the core will show a bounce and an outward shock will be the onset to the supernova explosion. The result is that most of the original iron core is photodisintegrated and a small core which is dominated by neutrons remains. Depending on whether the neutron-degeneracy pressure can withstand the extreme gravity or not, either a neutron star will stabilize or the core will collapse into a black hole. While this is happening the outside world is able to see the fireworks in the form of a type-II, type-Ib or type-Ic supernova explosion. For a short period of time the exploding star is as bright as the whole galaxy in which it appears.

For binary systems it is also possible to form neutron stars from white dwarfs. There are two formation possibilities. One way is by accretion-induced collapse, the other way by collapse after merging two white dwarfs. Both cases will result in an electron-capture type-Ia supernova if the mass of the white dwarf exceeds the Chandrasekhar critical mass.

For some excellent reading material on supernovae, neutron-star formation and nucleosynthesis see e.g. Shapiro & Teukolsky (1983), Burrows & Lattimer (1986), Burrows et al. (1995), Woosley & Weaver (1995), Woosley et al. (2002) and Lattimer & Prakash (2004).

1.3 Neutron-star basics

The inner structure of a neutron star described by the equation of state (EOS, i.e. the relationship between density and pressure) is still an open question in neutron-star astrophysics. A variety of neutron-star EOSs predict very different neutron-star mass-radius relations. Therefore, this relation is subject to many observational studies. Recent reviews by e.g. Lattimer & Prakash (2007) and Weber et al. (2007) give excellent insights into the current status and difficulties in the quest for the EOS.

In this thesis a canonical neutron star is sometimes used for first order estimates. This canonical neutron star has a mass M of 1.4 $\mathrm{M}_\odot$ (where $\mathrm{M}_\odot = 1.98892 \times 10^{33}$ g is the Solar mass) and a radius R of 10^6 cm = 10km. The moment of inertia $I = kMR^2 = 10^{45}\,\mathrm{g\,cm^2}$ is often used, which is a value between the moments of inertia of a solid sphere ($k = 2/5$) and a thin shell ($k = 2/3$).

If a neutron star does not accrete, it generally slows down. The kinetic energy loss for a certain pulse period (P), period derivative ($\dot{P}$) and moment of inertia (I) yields the spin-down luminosity of the pulsar.

$$\dot{E} = -\frac{\mathrm{d}}{\mathrm{d}t}\frac{1}{2}I\Omega^2 = -I\Omega\dot{\Omega} = I \cdot \frac{2\pi}{P} \cdot \frac{2\pi\dot{P}}{P^2} = 4\pi^2 I \frac{\dot{P}}{P^3} \simeq 3.95 \times 10^{46}\frac{\dot{P}}{P^3}\ [\mathrm{erg\,s^{-1}}] \tag{1.4}$$

For radio pulsars the bulk of this energy is not emitted in the form of radio emission, but in the form of energetic particles (pulsar wind) and high-energy radiation. In the magnetic dipole model (Pacini 1967, 1968; Gunn & Ostriker 1969) for an oblique rotator in a vacuum with a magnetic dipole moment **m** with

$$|\mathbf{m}| = \frac{BR^3}{2}, \tag{1.5}$$

where B is the surface magnetic-field strength, the pulsar radiates magnetic energy at the rate

$$\dot{E} = \frac{2|\mathbf{m}|^2\Omega^4 \sin^2\alpha}{3c^3}\ [\mathrm{erg\,s^{-1}}] \tag{1.6}$$

where c is the speed of light and α the angle between the rotation axis and the magnetic polar axis.

If one assumes that the spin down of the neutron star is caused by the torque of the magnetic field with its surroundings and that the emission process is dipole radiation, one can infer a characteristic surface magnetic field (at the poles) by equating Eq. 1.4 (applying Eq. 1.5) with Eq. 1.6

$$B = \sqrt{\frac{3c^3 I}{2\pi^2 R^6 \sin^2\alpha} P\dot{P}} = 6.4 \times 10^{19}\sqrt{P\dot{P}}\ [\mathrm{G}]. \tag{1.7}$$

As α is usually not known, the magnetic field strength at the equator is more commonly used as a characteristic value, which is half of the field at the poles, and $\sin^2\alpha = 1$ is assumed,

yielding

$$B = 3.2 \times 10^{19} \sqrt{P\dot{P}}\,[\mathrm{G}]. \tag{1.8}$$

Noteworthy is the so-called critical magnetic field strength (also sometimes called $B_{\mathbf{QED}}$);

$$B_{\mathrm{cr}} = \frac{m_e^2 c^3}{e\hbar} = 4.413 \times 10^{13}\,[\mathrm{G}]. \tag{1.9}$$

This is the magnetic field at which the mass of the electron equals the first Landau excitation energy. Quantum electrodynamic (QED) physics around and above this critical magnetic field is playing an important role (see e.g. Duncan 2000). QED effects include that the vacuum becomes anisotropic and it becomes birefringent (comparable with the double refraction in e.g. a calcite crystal) causing vacuum polarization. The light will become decomposed in ordinary (O) and extraordinary (E) photons and can cause magnetic lensing. Another QED effect is photon splitting (and merging, see e.g. Adler 1971; Harding et al. 1997) which is dominated by $E \rightarrow O + O$. Photon-electron scattering will be strongly suppressed in the E mode. Atoms in these high magnetic fields are distorted into long thin cylinders (see e.g. Lai 2001).

Assuming a spin-down formula $\dot{\nu} \propto \nu^n$ where n is the breaking index and $\nu(= 1/P)$ the spin frequency, one can calculate the age of the pulsar (assuming no temporal distortions). By integrating the spin-down formula one finds

$$\tau = \frac{P}{(n-1)\dot{P}} \left[1 - \left(\frac{P_0}{P} \right)^{n-1} \right]\,[\mathrm{s}]. \tag{1.10}$$

If one assumes the pulse period at birth (P_0) is much smaller than the current pulse period and the breaking index equals three (i.e. dipole radiation), then the commonly used expression for the characteristic age is found

$$\tau_c = \frac{P}{2\dot{P}}\,[\mathrm{s}]. \tag{1.11}$$

The characteristic age should always be considered as a first order estimate as deviations from the real age can be significant. In reality pulsars may have other ways of energy dissipation, the 'vacuum' condition is definitely not valid for (young) pulsars and pulsars occasionally do show temporal distortions.

That a neutron star can not be surrounded by a vacuum was first shown (with a contradiction argument) by Goldreich & Julian (1969). A rotating magnetic dipole surrounded by a vacuum will induce a Lorentz force parallel to the magnetic field. For pulsars (B and P) this force will exceed the gravitational force by orders of magnitude. Charged particles will be lifted from the surface into the magnetosphere. The particles will co-rotate with the neutron star within the light cylinder magnetosphere. Along the open field lines particles will stream across the light cylinder. A force-free magnetosphere is possible if the Goldreich-Julian charge density is reached. However, just as a vacuum this will also not be physical as then currents would not exist, no particle acceleration and therefore also no radiation. Moreover, in the

magnetosphere electron-positron pairs are produced by the photons which are radiated by the accelerated particles lifted from the surface. A force-free magnetosphere will not exist in reality, however, it is assumed in many atmosphere/magnetosphere models.

Electro-magnetic radiation can be created at different sites. Popular models are the polar-cap models which include the vacuum-gap model (Ruderman & Sutherland 1975; Usov & Melrose 1995) and the space-charge limited-flow gap model (Usov & Melrose 1995; Harding & Muslimov 1998), slot-gap model (Arons 1983; Muslimov & Harding 2003) and outer-gap model (Cheng et al. 1986; Romani 1996; Hirotani 2006). These are named after the sites where particle acceleration can be efficient due to an electric field parallel to the magnetic field. For the observed non-thermal emission ranging from radio to the gamma-ray domain emission mechanisms like curvature radiation, synchrotron radiation or (inverse) Compton scattering play a role.

1.4 Isolated neutron stars

Considering that about 1% of all stars end up as neutron stars means that there are many neutron stars in the Universe. Of the $\sim 10^{8-9}$ neutron stars in our Galaxy only $\sim$2000 are detected, most as pulsars. These numbers show how elusive these objects are.

While it is thought that all neutron stars have the same EOS (Weber et al. 2007; Lattimer & Prakash 2007), neutron stars exhibit vastly different kinds of behaviour. Neutron stars can either be isolated or they can be part of a binary/multiple system. Either way, the neutron star could show itself as a pulsar. In general the pulsar can be powered thermally, magnetically, or by rotation or accretion.

Given the contents of this thesis I shortly introduce the isolated neutron stars.

Isolated Neutron Stars (INSs) represent the bulk of the known neutron stars. Out of the $\sim$1800 non-accreting pulsars that are known to date $\sim$1650 are isolated neutron stars. Most of these $\sim$1800 pulsars are rotation-powered radio pulsars (ATNF pulsar catalog; Manchester et al. 2005), with rotation periods ranging from 0.1 s to 2 s and magnetic fields clustering around 10^{11-13} G (assuming Eq. 1.8, see Fig. 1.1). From most of them only radio emission is detected, however some of them also emit in X-rays and some even show gamma-ray emission. They are generally very stable rotators, some of them are even more stable than the best atomic clocks on Earth. Summarizing everything what has been found in 40 years of pulsar astrophysics is impossible and far beyond the scope of this thesis, therefore I refer to some excellent/classic books by Manchester & Taylor (1977) and Lorimer & Kramer (2004).

Another class of INSs are the magnetars. Currently there are 13 magnetars known (+ 2 candidates). There are two groups of sources which belong to the magnetar class, the anomalous X-ray pulsars (9 + 1) and the soft gamma-ray repeaters (4 + 1). They are slowly rotating pulsars with spin periods ranging from 2 s to 12 s. They have large period derivatives on the order of $10^{-10} - 10^{-13}$s s^{-1} and therefore strong magnetic fields are inferred (10^{14-15} G, see Eq. 1.8). These properties place these objects in the upper right of the $P - \dot{P}$ diagram (see Fig. 1.1). Their characteristic ages, locations close to the Galactic plane (see Fig.1.2) and

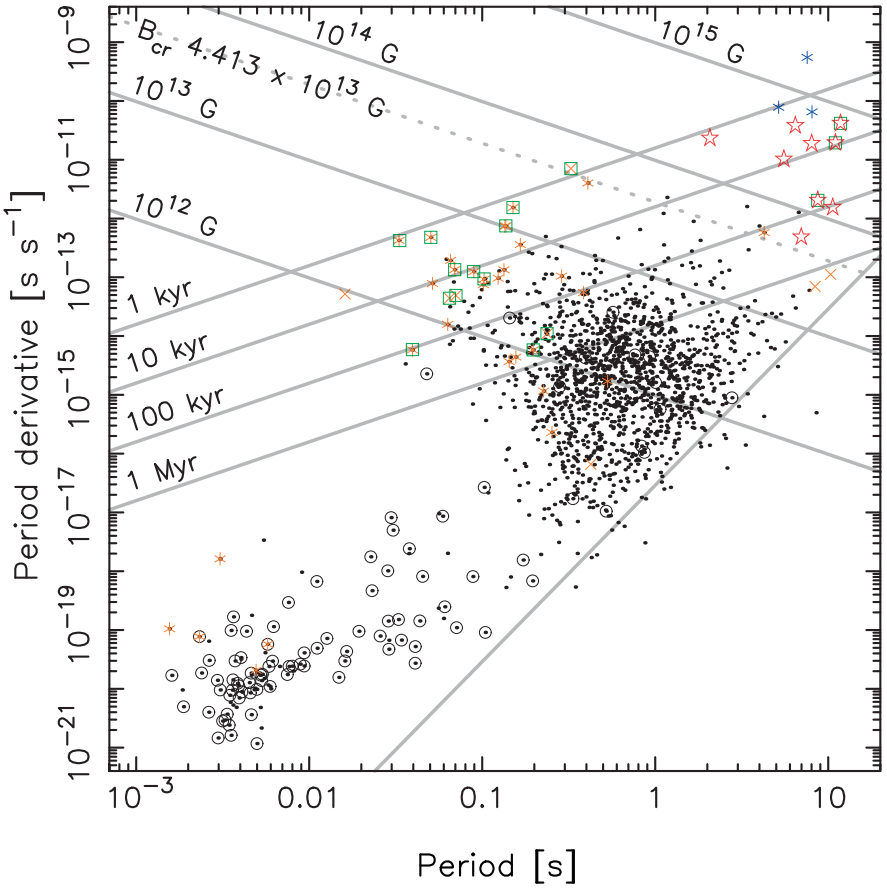

Figure 1.1: *$P-\dot{P}$ (period vs. period derivative) diagram of all known pulsars (with measured $P-\dot{P}$) which are not powered by accretion. The black dots indicate all rotation-powered radio pulsars. The pulsars in a circle are in binary systems. The orange symbols are high-energy pulsars. The orange stars indicate pulsars which show pulsed emission from radio up to X-rays and the crosses are radio-dim high-energy pulsars. With green squares are the pulsars indicated for which pulsed emission has been detected above ∼50 keV. In the upper right part of this diagram the magnetars are found. The three SGRs with known period derivatives are indicated with blue stars and the nine AXPs are indicated with red stars. In grey are indicated the lines of equal characteristic age ($\tau_c = P/2\dot{P}$) and equal dipole magnetic field strength ($B \sim 3.2\times10^{19}\sqrt{P\dot{P}}$ G, $B_{\rm cr} = m_e^2c^3/e\hbar = 4.413\times10^{13}$ G). Also indicated with a grey line is the/a pulsar death line below which pulsars 'should' not be able to produce radio emission (Ruderman & Sutherland 1975). Data from the online ATNF pulsar catalog are used in this figure (http://www.atnf.csiro.au/research/pulsar/psrcat/; Manchester et al. 2005).*

some associations with supernova remnants indicate they form a young population. The magnetars are thought to be magnetically powered as the high-energy luminosity is/can be orders of magnitude larger than the maximum luminosity released through rotation power (Eq 1.4). See Sect. 1.5 for a detailed description.

Interestingly, there are a handful of radio pulsars that also have very high magnetic fields (e.g. Camilo et al. 2000; Morris et al. 2002; McLaughlin et al. 2003; Hobbs et al. 2004a; McLaughlin et al. 2007). These high-field radio pulsars have inferred magnetic fields (assuming Eq. 1.8) higher than $B_{\rm cr} = 4.413 \times 10^{13}$ G (see Eq. 1.9 and Fig. 1.1). Finding radio pulsars with these high magnetic fields is remarkable as it was expected that no radio emission could be produced close to/above $B_{\rm cr}$ due to suppression of the electron-positron pair production by photon splitting (Baring & Harding 1998). Some of these pulsars even have higher magnetic fields than the lowest-magnetic-field magnetar (see Fig. 1.1). One might expect some magnetar-like behaviour of these pulsars (see Sect. 1.5), but this has not been observed so far. For example, their X-ray luminosities are orders of magnitude lower than the ones found for magnetars (e.g. Pivovaroff et al. 2000; Kaspi & McLaughlin 2005; Gonzalez et al. 2005) and also no bursts have been detected yet.

However, surprising behaviour has been reported from the rotation-powered X-ray pulsar PSR J1846-0258 ($P = 324$ ms; $\dot{P} = 7.1 \times 10^{12}\,{\rm s\,s^{-1}}$). This pulsar is located at the centre of supernova remnant Kes 75 (G29.6+0.1 Gotthelf et al. 2000) and so far no radio emission is detected. This high magnetic field ($B \sim 4.9 \times 10^{13}$ G) X-ray pulsar is one of the youngest pulsars with a characteristic age $\tau_c = 723$ yr. In 2006 it has shown an outburst where it brightened almost an order of magnitude (Kumar & Safi-Harb 2008). Also a pulsed-flux brightening has been observed for $\sim$50 days during which also 5 magnetar-like bursts were detected (Gavriil et al. 2008b). While PSR J1846-0258 has a high $\dot{E} = 8.2 \times 10^{36}\,{\rm erg\,s^{-1}}$ and its X-ray luminosity remained well below this value, it did show magnetar-like behaviour (see Sect. 1.5). Moreover, for this pulsar hard pulsed X-ray emission has been detected Kuiper & Hermsen (2008). With the current spin down (Livingstone et al. 2007) this pulsar will enter the magnetar region in the $P - \dot{P}$ diagram (Fig. 1.1) within a few ten-thousand years. This source might provide valuable information linking the rotation-powered pulsars to the magnetars, or about the early evolution of magnetars.

Of particular interest are 7 radio-dim INSs (called the magnificent seven for many years, however, recently an eighth candidate has been discovered; Rutledge et al. 2008) which were discovered in the ROSAT All-Sky Survey (Voges et al. 1999). The X-ray spectra are purely thermal ($kT \sim 0.04 - 0.1$ keV) with broad absorption lines (see Haberl 2007, for a review). If these spectral lines are caused by cyclotron absorption, the magnetic field strengths of these objects are either $\sim 10^{10-11}$ G or $\sim 10^{13-14}$ G depending on whether this absorption is caused by electrons or protons, respectively. Therefore, they are excellent candidates for studying neutron-star atmospheres and the EOS (e.g. Paerels 1997; Pons et al. 2002). They are slow rotators with pulse periods $P \sim 3.5 - 11.5$ s and small pulsed fractions. Recent period-derivative measurements ($\dot{P} \sim 10^{-13}\,{\rm s\,s^{-1}}$ Kaplan & van Kerkwijk 2005a,b; van Kerkwijk & Kaplan 2008) yield magnetic field strengths $B \sim 2 - 3 \times 10^{13}$ G and characteristic ages

of $\sim 1 - 2 \times 10^6$ yr (assuming Eqs. 1.8 & 1.11). This could indicate that the lines are due to cyclotron absorption by protons. However, atmosphere models are also capable of producing similar line features in a high magnetic field (e.g. van Kerkwijk & Kaplan 2007; Pons et al. 2007). The radio-dim INSs have characteristic ages larger than the magnetars, but the high magnetic-field strengths could indicate that they might be the evolutionary descendants of the magnetars (see e.g. Haberl 2007).

While the magnificent seven might be the evolutionary late type magnetars, the Central Compact Objects (CCOs) might be the younger relatives of magnetars (De Luca 2008). CCOs form a group (currently $\sim$7) of young ($\tau_c < 7$ kyr, Eq. 1.11) neutron stars in the centres of supernova remnants (Pavlov et al. 2004). One of them is the compact object embedded in Cassiopeia A, the youngest supernova remnant of our Galaxy to date. Like the magnificent seven and most magnetars, CCOs are radio dim. Their X-ray spectra are thermal-like with temperatures $kT \sim 0.2 - 0.5$ keV while some also need a soft power-law component ($\Gamma > 2$) to describe their spectra. On the other hand Gotthelf & Halpern (2008) found evidence that CCOs might be neutron stars born with a very low magnetic field, contrary to the magnetars. This would be in agreement with the lack of pulsar-wind nebulae, which points towards a low $\dot{E}$ and therefore low magnetic field.

Finally, a few words on gamma-ray pulsars (see Fig. 1.1). Currently there are six gamma-ray pulsars for which pulsed emission above $\sim$100 MeV has definitely been detected. This small sample has been used to study particle acceleration and high-energy emission mechanisms in pulsar magnetospheres. Among these, Geminga (PSR J0633+1746 Fichtel et al. 1975) is one of the brightest gamma-ray sources in the sky at energies above $\sim$100 MeV (for a recent high-energy study see Jackson et al. 2002, and references therein). However, Geminga either does not emit in the radio waveband or the radio beams miss the Earth, contrary to the other 5 gamma-ray pulsars ($>$100 MeV) like the Crab pulsar. In the hard X-ray range ($>$50 keV) only three pulsars were detected until recently. This number has now more than doubled (presented by Kuiper in Montreal 2007). These hard X-ray pulsars are radio dim (two are quiet) and are good candidates to be picked up with future high-energy gamma-ray observatories. They are young pulsars ($<$100 kyr) with high $\dot{E}$ which can power pulsar-wind nebulae.

A consensus in the identification scheme of neutron stars is not reached yet. It is likely that some of the INS manifestations could be explained by different phases in the evolution. However, it is also possible that the birth properties of one type of neutron star are indeed significantly different from those of another type and that therefore different types of neutron stars will follow completely different evolutionary tracks.

1.5 Magnetars

Having briefly discussed the different manifestations of neutron stars, now in more detail the magnetar will be introduced. The Soft Gamma-ray Repeaters (SGRs) and the Anomalous X-ray Pulsars (AXPs) are the two groups of (isolated) neutron stars which belong to the magnetar

class. They are slowly rotating ($P \sim 2 - 12$ s) with large period derivatives ($\dot{P} \sim 10^{-10} - 10^{-13}\,\mathrm{ss}^{-1}$) and therefore they have very high inferred magnetic field strengths on the order of 10^{14-15} G (see Eq. 1.8). Their characteristic ages, locations close to the Galactic plane (see Fig. 1.2) and some associations with supernova remnants indicate that they form a young neutron-star population. Currently 13 magnetars (+ 2 candidates) are known; 9 (+ 1) AXPs and 4 (+ 1) SGRs. The magnetar model is proposed to describe the observed characteristics of SGRs and AXPs. First, the SGRs are introduced in a historical perspective based on observations. Then a description of the magnetar model follows. Finally, the AXPs will be introduced in more detail, as they form the main research topic of this thesis

1.5.1 Soft gamma-ray repeaters

The first event from a Soft Gamma-ray Repeater (SGR; see Tables 1.1 and 1.2 for some characteristics) was detected on January 7, 1979 (Mazets & Golenetskii 1981; Laros et al. 1986; Aptekar et al. 2001). This burst originated from SGR 1806-20, even though the first published position was wrong. It was detected by one of the KONUS experiments onboard one of the *Venera* satellites which were looking for Gamma-Ray Bursts (GRBs; extremely luminous cosmic explosions). Soon thereafter, on March 5, 1979 an extraordinary bright event was observed (Mazets et al. 1979). It had an initially extremely bright spike and a 3-minute decaying tail in which 8-second pulsations were visible. The energy released during this burst was enormous i.e. $\sim 5 \times 10^{44}$ erg (assuming isotropic emission). It was the first of three giant flares detected from SGRs so far. The source is currently known as SGR 0526-66 and is located in the Large Magellanic Cloud (Cline et al. 1982). Within a day another burst was detected from SGR 0526-66 (Mazets & Golenetskii 1981). This one was orders of magnitude less intense (Aptekar et al. 2001). Another recurrent burster was discovered when on March 24, 25 and 27 1979 three soft short bursts were detected from the same location (SGR 1900+14). These bursts were first classified as strange soft GRBs. At that time GRB research was also still in its early days, only a few years after the discovery of the first GRB (Klebesadel et al. 1973). Moreover, before the above-mentioned events a GRB has never been observed from the same location more than once. It is remarkable that the first three out of the currently four (+ 1 candidate) known SGRs were discovered within three months from each other. All three bursters, SGR 0526-66, SGR 1900+14 and SGR 1806-20 showed recurrent bursting activity (Golenetskii et al. 1984; Atteia et al. 1987; Laros et al. 1987; Kouveliotou et al. 1987) and the name soft gamma-ray repeater was born.

Of great importance in SGR and magnetar astrophysics in general was the discovery of the period and period derivative in the persistent X-ray emission of SGR 1806-20 by Kouveliotou et al. (1998). They noticed that the persistent X-ray flux from SGR 1806-20 is two orders of magnitude higher than the energy available in spin-down energy (Eq. 1.4). Moreover, these measurements indicate a magnetic field of $\sim 8 \times 10^{14}$ G (Eq. 1.8). They argue that the energy production is due to the decay of an extremely high magnetic field as was already proposed in the magnetar model (see Sect. 1.5.2).

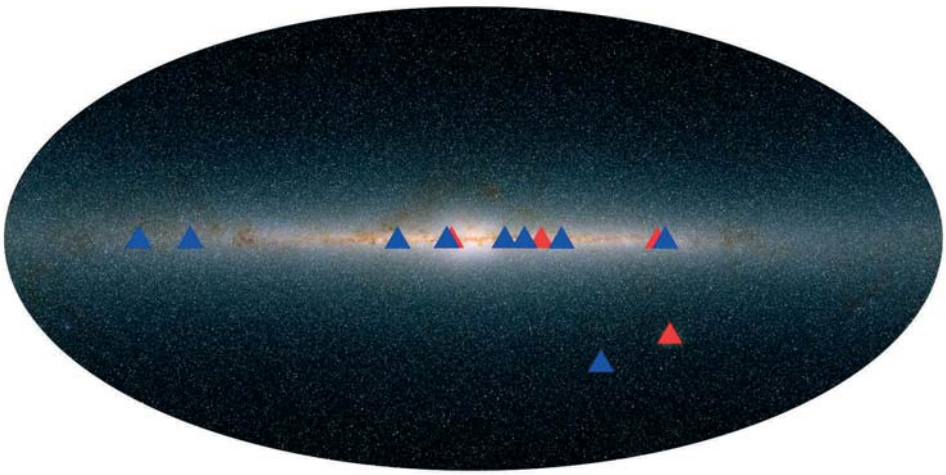

Figure 1.2: *Two Micron All-Sky Survey image mosaic with the locations of the magnetars. AXPs are indicated in blue and SGRs are indicated in red. Except for the two sources in the Magellanic clouds the magnetars are distributed close to the Galactic plane. Image credit: J. Carpenter, T. H. Jarrett, & R. Hurt; Image mosaic obtained as part of the Two Micron All Sky Survey (2MASS), a joint project of the University of Massachusetts and the Infrared Processing and Analysis Center/California Institute of Technology.*

The bursting behaviour of SGRs is very irregular. SGRs tend to have episodes of bursting activity. During these episodes hundreds of bursts can be seen within several weeks. It can also occur that an SGR does not show any bursts for years. For example, no bursts have been detected from SGR 0526-66 since 1983, and SGR 1627-41 showed only one bursting episode of six weeks in which 99 bursts have been detected (Woods et al. 1999b). The most common bursts have durations of $\sim$0.04–1.0 s with the peak of the distribution around 0.1–0.2 s (Aptekar et al. 2001; Göğüş et al. 2001). But, occasionally longer and more intense bursts are observed. Detections of some weak spectral features were claimed for some SGR bursts, which might be cyclotron features (Strohmayer & Ibrahim 2000; Ibrahim et al. 2003).

Interestingly, Cheng et al. (1996) noticed that the energy distribution of the bursts from SGR 1806-20 is a power-law ($dN/dE \propto E^{-5/3}$) which looks remarkably similar to the Gutenberg-Richter law for earthquakes (Gutenberg & Richter 1956). Also, the waiting times for the earthquakes and the SGR bursts are comparable. Moreover, neither earthquakes nor SGR bursts show a correlation between energy and waiting time.

The spectra of SGR-bursts are very different from spectra from other transient events like e.g. GRBs. The SGR-burst spectra can (usually) be described with double black-body models (e.g. Feroci et al. 2004; Nakagawa et al. 2007). They have hard spectra up to the spectral break after which they decay fast. X-ray bursts from X-ray binary sources are much softer and

do not reach energies as high as SGR bursts. GRBs do have high-energy photons but their spectra do not decay as fast after their spectral breaks (see Fig. 14.5 in Woods & Thompson 2006).

The persistent X-ray spectra ($<$10 keV) from SGRs are power-law like ($\Gamma \sim 2-3$) with in some cases a small thermal black-body component (e.g. Kulkarni et al. 2003; Kouveliotou et al. 2003; Woods et al. 2007; Esposito et al. 2007). So far, no spectral features have been detected. The unabsorbed 2–10 keV fluxes range from 10^{-13} to 10^{-11} erg cm^{-2} s^{-1}. Recently, persistent hard X-ray emission ($>$20 keV) has been detected from SGR 1806-20 and SGR 1900+14 with INTEGRAL (Mereghetti et al. 2005a; Molkov et al. 2005a; Götz et al. 2006; Esposito et al. 2007). These spectra are also power-law like with photon indices $\Gamma = 1.5-1.9$ (Mereghetti et al. 2005a) and $\Gamma = 1.6$ (Molkov et al. 2005a) for SGR 1806-20 and for SGR 1900+14 $\Gamma = 3.1$ (Götz et al. 2006) and $\Gamma = 1.6$ (Esposito et al. 2007).

Especially SGR 1900+14 and SGR 1806-20 are exiting systems. SGR 1900+14 showed a giant flare on August 27, 1998 (Hurley et al. 1999) which was very similar to the giant flare from SGR 0526-66. On December 27, 2004, INTEGRAL discovered (Borkowski et al. 2004) a giant flare ($\sim 10^{47}$ erg) from SGR 1806-20 more than two orders of magnitude brighter than the two previously measured giant flares. The X-rays from both giant flares ionized the Earth's upper atmosphere, changing the radio propagation properties of the Earth's ionosphere (Inan et al. 1999; Campbell et al. 2005; Mandea & Balasis 2006; Inan et al. 2007). After both flares radio afterglows were observed (Frail et al. 1999; Cameron et al. 2005; Gaensler et al. 2005a). The afterglow of SGR 1806-20 was monitored intensively and the radio afterglow shell was expanding, polarized and showed rebrightening (Gaensler et al. 2005a; Gelfand et al. 2005; Taylor et al. 2005).

The pulse profiles of SGR 1806-20 and SGR 1900+14 showed significant morphology changes, especially after the giant flares. Before the giant flare SGR 1900+14 showed a complex pulse profile with at least three different components. After the giant flare the pulse profile changed within a few minutes to sinusoidal-like and thus single peaked (Woods et al. 1999a, 2001). Also, more long-term and smooth pulse-profile morphology changes have been observed for both SGR 1806-20 and SGR 1900+14 (Göğüş et al. 2002; Tiengo et al. 2005a).

The increases in pulse periods of SGR 1900+14 and SGR 1806-20 showed deviations from constant spin down (Kouveliotou et al. 1999; Woods et al. 2000). This can be attributed to significant timing noise which is larger than generally seen for radio pulsars (Arzoumanian et al. 1994). Timing noise is particularly apparent in young pulsars and correlates with $\dot{P}$. It is associated with different kinds of torque variations (Boynton et al. 1972; D'Alessandro 1996, e.g.). Contrary to a glitch (a sudden increase in pulse frequency), timing noise can result in a more gradual drift of the timing parameters. Both SGR 1900+14 and SGR 1806-20 have shown large and long-term torque variations (Woods et al. 2002, 2007).

Very interesting is the discovery of different quasi periodic oscillations in the tails of the giant flares of SGR 1806-20, SGR 1900+14 and maybe also SGR 0526-66 (Israel et al. 2005b; Strohmayer & Watts 2005, 2006; Watts & Strohmayer 2006; Barat et al. 1983) which might be explained by oscillation modes of the crust. From these oscillations Vietri et al. (2007)

estimated a lower limit to the magnetic-field strength of $\sim 10^{15}$ G, independent of the dipole magnetic field estimate.

1.5.2 Magnetar model

'Why do almost all radio pulsars have magnetic fields of about 10^{12} Gauss?' This is what Duncan and Thompson were asking themselves in 1986 (Duncan 2005). What they found was a big surprise. Neutron stars could have extreme surface magnetic fields up to 10^{15} G. Only in the early nineties – after years of checking their calculations – they 'dared' to publish their findings (Duncan & Thompson 1992; Thompson & Duncan 1993). Nowadays with all the observational evidence, the majority of the scientific community is convinced that the magnetar model is viable.

Duncan and Thompson launched their idea on how highly magnetized neutron stars could form and how they could explain a number of observed properties of SGRs in the early nineties (Duncan & Thompson 1992; Thompson & Duncan 1993). They studied how effective a dynamo action can be within a short period of convection during the formation of the proto neutron-star (c.f. Burrows & Lattimer 1986). The dynamo effect (comparable to the solar dynamo at a different scale) will be active only for a few seconds, but this can be sufficient to boost the internal (toroidal) magnetic field up to $B \sim 10^{16}$ G (see Thompson & Duncan 1993, and references therein for a detailed description of the dynamo effect and comparison with the Sun).

The dynamo is only effective within a small range of initial birth parameters like a short (few ms) rotation period. Therefore, this mechanism is debated and other processes to reach magnetar fields are proposed. One of them is by flux conservation from a fossil field of the massive O-B-A star progenitor of the neutron star (see for recent work e.g. Ferrario & Wickramasinghe 2005, 2006, 2007a,b). Another hypothesis is field amplification by differential rotation and a magnetic instability (e.g. Spruit 2002; Akiyama et al. 2003). All three mechanisms can possibly generate magnetar-like field strengths, but also all three have their difficulties and uncertainties (e.g. Spruit 2008). A completely new approach with a different (and testable) evolutionary track for magnetars was recently proposed by Bhattacharya & Vikram (2008) (see below). They propose (nuclear) spin alignment in a strongly interacting environment. This scenario involves pion-condensate quark matter for which they explored two EOSs.

The birth mechanism and origin of the magnetic field for neutron stars and magnetars in particular are important to understand, but they are of less importance for explaining the current observed characteristics. Nevertheless, it is clear that it is theoretically possible to create neutron stars with magnetar fields.

Important to realize is that magnetars differ from radio pulsars because the dominating energy source is magnetic dissipation in magnetars and rotation in spin-down powered pulsars. The toroidal magnetic field contains a huge internal energy reservoir. The involved magnetic fields are above the critical magnetic field $B > B_{\rm cr} = 4.413 \times 10^{13}$ G (Eq. 1.9). Therefore, the

local physics is difficult and involves photon splitting (and merging), vacuum becoming birefringent (like a calcite crystal), vacuum polarization and atom deformations to long spaghetti-like cylinders (e.g. Duncan 2000; Adler 1971; Lai 2001).

Goldreich & Reisenegger (1992) explored possible mechanisms of magnetic energy transport from the core to the surface. Mechanisms that are involved are Ohmic dissipation, ambipolar diffusion and Hall drift. The dissipation of magnetic energy by Ohmic decay is possible, but it has a characteristic time scale which is too long to significantly contribute to this process in magnetars. One component of ambipolar diffusion is capable of transporting magnetic flux from the core to the lower crust. In the crust the Hall effect is the dominating factor. Hall drift does not dissipate magnetic energy (it is conservative), but in high magnetic-field regimes it is possible to get Hall turbulence which enhances the local rate of Ohmic dissipation. The force due to the magnetic field (which is anchored in the crust and undergoes Hall drift; i.e. Goldreich & Reisenegger 1992; Pons & Geppert 2007) is likely to exceed the critical strength of the crust. A sudden rupture (Hall fracture) of the crust can give rise to a glitch and/or a burst. Magnetic fields of 10^{15} G are sufficient to power magnetar bursts including the extremely intense giant flares. The field can also confine a cooling plasma over the duration of giant-flare tails (Duncan & Thompson 1992; Duncan 2004; Paczyński 1992; Thompson & Duncan 1995, 1996).

In this scheme, Thompson & Duncan (1995, 1996) modeled the magnetar in great detail. Full derivations of boundary conditions, energetics, physical mechanisms and time scales are given, for both the bursting as well as the stable domain. The internal and external conditions of the magnetar are explored for magnetic fields stronger than $\sim 10^2 B_{\rm cr}$, including radiative transport within the QED regime. This is compared with the observed SGR characteristics. Also different (i.e. non magnetar) mechanisms are discussed.

A breakthrough for the magnetar model was undoubtedly the first P and $\dot{P}$ measurement from persistent emission from SGR 1806-20 (Kouveliotou et al. 1998) which placed this pulsar in the high magnetic-field region in the $P-\dot{P}$ diagram (Fig. 1.1). Moreover, the X-ray luminosity exceeding the available spin-down power (see Eq. 1.4) by two orders of magnitude was in favour of the proposed powering mechanism by magnetic decay. Also the sudden pulse-profile morphology change observed from SGR 1900+14 (Thompson et al. 2000; Woods et al. 2001) was in support of the magnetar model as this can be interpreted as evidence for a sudden change in magnetic-field configuration.

To better understand and explain persistent emission and torque behaviour, the magnetar model was expanded by Thompson et al. (2002). The authors explored the effects of the internal twisted (toroidal) magnetic field on the external (poloidal) magnetic-field structure. They found that the internal field ($\sim 10^{15-16}$ G) is strong enough to twist also the external magnetic field. The twist induces currents which are responsible for (black-body) surface heating and non-thermal persistent emission (< 10 keV). The external twist will increase the spin-down torque (higher $\dot{P}$) of the neutron star as the twist will cause extra magnetospheric current to cross the light cylinder. A larger twist will cause a harder spectrum (positive hardness vs spin-down correlation). Moreover, the energy reservoir of $\sim 10^{47} B_{15}^2$ erg (where B_{15} is in units

Table 1.1: *Magnetar characteristics.: pulse period P, period derivative $\dot{P}$, surface magnetic field strength B (see Eq. 1.8), characteristic age τ_c (see Eq. 1.11) and distance d. Adapted from Woods & Thompson (2006) and SGR/AXP online catalog http://www.physics.mcgill.ca/pulsar/magnetar/main.html*

Object	P s	$\dot{P}$ $\times 10^{-11}$ s s^{-1}	B $\times 10^{14}$ G	τ_c kyr	d kpc
SGR 0526-66	8.05	6.5	7.3	2.0	50
SGR 1627-41	6.4$^{?}$				
SGR 1801-23$^{(1)}$					
SGR 1806-20	7.56	54.9	21	0.22	15
SGR 1900+14	5.17	7.78	6.4	1.1	12–15
CXOU J010043.1-721134	8.02	1.88	3.9	6.8	57
4U 0142+61	8.69	0.20	1.3	70	3.6
1E 1048.1-5937	6.45	2.70	4.2	3.8	9
1E 1547.0-5408	2.07	2.32	2.2	1.4	4/9
CXOU J164710.2-455216	10.61	0.16	1.3	108	4
1RXS J1708-40	11.00	1.95	4.7	9.0	3.8
XTE J1810-197	5.54	0.81	1.7	17	2.5
1E 1841-045	11.78	4.16	7.1	4.5	6.7
AX J1845.0-0258$^{(1)}$	6.97				$<$20
1E 2259+586	6.98	0.048	0.6	230	7.5

[1] Magnetar candidate; [?] Likely pulse period.

References e.g.: **0526** – Kulkarni et al. (2003); Klose et al. (2004); **1627** – Woods et al. (1999b); Corbel et al. (1999); **1801** – Cline et al. (2000); **1806** – Mereghetti et al. (2005c); Corbel & Eikenberry (2004); **1900** – Woods et al. (2002); Vrba et al. (2000); **0100** – McGarry et al. (2005); Lamb et al. (2002); **0142** – Gavriil & Kaspi (2002); Durant & van Kerkwijk (2006a); **1048** – Kaspi et al. (2001); Durant & van Kerkwijk (2006a); **1547** – Camilo et al. (2007b); Gelfand & Gaensler (2007); **1647** – Muno et al. (2006); Woods et al. (2006); Kothes & Dougherty (2007); **1708** – Gavriil & Kaspi (2002); Durant & van Kerkwijk (2006a); **1810** – Halpern & Gotthelf (2005); Gotthelf & Halpern (2005); **1841** – Gotthelf et al. (2002); Vasisht & Gotthelf (1997); **1845** – Torii et al. (1998); Gaensler et al. (1999); **2259** – Gavriil & Kaspi (2002); Durant & van Kerkwijk (2006a).

Table 1.2: *Magnetar characteristics: Detections (+) in radio, Optical, Near InfraRed, X-rays (<10 keV) and hard X-rays (>20 keV), or transient phenomena.*

Object	Radio	Opt/NIR	X	hard X	Glitch	Bursts	Giant Flare
SGR 0526-66	–	–	+	–	–	+	+
SGR 1627-41	–	–	+	–	–	+	–
SGR 1801-23[1]	–	–	+	–	–	+	–
SGR 1806-20	±[2]	–/+	+	+	–	+	+
SGR 1900+14	±[2]	–	+	+	–	+	+
CXOU J01004-7211	–	+/–	+	–	–	–	–
4U 0142+61	–	+/+	+	+	+[?]	+	±[3]
1E 1048.1-5937	–	+/+	+	–	+	+	±[3]
1E 1547.0-5408	+	–	+	–	–	–	–
CXOU J16471-4552	–	–	+	–	+	+	–
1RXS J1708-40	–	–/+	+	+	+	–	–
XTE J1810-197	+	–/+	+	–	–	+	±[3]
1E 1841-045	–	–	+	+	+	–	–
AX J1845.0-0258[1]	–	–	+	–	–	–	–
1E 2259+586	+	–/+	+	+[?]	+	+	–

[1] Magnetar candidate; [2] Radio afterglow after giant or bright flare; [3] Large AXP flare with some SGR giant flare characteristics; [?] Likely detection.

References e.g.: **0526** – Kulkarni et al. (2003); Aptekar et al. (2001); Mazets et al. (1979); **1627** – Mereghetti et al. (2006a); Woods et al. (1999b); **1801** – Cline et al. (2000); **1806** – Cameron et al. (2005); Gaensler et al. (2005a); Israel et al. (2005a); Mereghetti et al. (2005c,a,b); Molkov et al. (2005a); Götz et al. (2004); **1900** – Frail et al. (1999); Mereghetti et al. (2006b); Esposito et al. (2007); Feroci et al. (2004); Hurley et al. (1999); **0100** – Durant & van Kerkwijk (2005a, 2008); McGarry et al. (2005); **0142** – Hulleman et al. (2000); Durant & van Kerkwijk (2006c); Patel et al. (2003); Kuiper et al. (2006); den Hartog et al. (2008a); Morii et al. (2005b); Gavriil et al. (2008a); **1048** – Wang et al. (2007); Durant & van Kerkwijk (2005b); Tiengo et al. (2005b); Dib et al. (2007b); Gavriil et al. (2006); **1547** – Camilo et al. (2008); Halpern et al. (2008); **1647** – Israel et al. (2007a); Muno et al. (2007); Krimm et al. (2006); **1708** – Durant & van Kerkwijk (2006d); Kuiper et al. (2006); den Hartog et al. (2008b); Dib et al. (2008a); **1810** – Kramer et al. (2007); Israel et al. (2004a); Gotthelf & Halpern (2005); Woods et al. (2005); **1841** – Morii et al. (2003); Kuiper et al. (2006); Dib et al. (2008a); **1845** – Tam et al. (2006); **2259** – Malofeev et al. (2005); Tam et al. (2004); Woods et al. (2004); Kuiper et al. (2006); Kaspi et al. (2003); Gavriil et al. (2004).

10^{15} G) is sufficient to power magnetars for several thousand years (assuming a luminosity of $\sim 10^{35}$ erg s^{-1}(Durant & van Kerkwijk 2006a)). It also explains why there are no old magnetars discovered. The absence of an internal energy reservoir in the form of a twisted magnetic field is thought to be the explanation why high magnetic-field radio pulsars do not show magnetar-like behaviour.

Finally, Bhattacharya & Vikram (2008) suggest a different evolutionary track of magnetars. A highly magnetic core can be created dynamically due to spin (vector) alignment in the strong-force regime. This high magnetic field is screened by currents in the neutron-proton-electron plasma surrounding the core. This magnetic configuration would be in a higher state than a relaxed dipolar state. The time scale to relax the field would be set by ambipolar diffusion (Goldreich & Reisenegger 1992). The surface magnetic field would gradually rise until it reaches magnetar strengths after $\sim 10^4$ yr. The expected luminosity would be $\sim 10^{35-36}$ erg s^{-1}due to the huge magnetic-field energy. The expected magnetar lifetime is $\sim 10^4$ yr. Observations of young high-magnetic-field radio pulsars like PSR J1119-6127 or X-ray pulsar PSR J1846-0258 (in Kes 75) could support this evolutionary scenario. According to this model scenario these sources may become magnetars in the future.

1.5.3 Anomalous X-ray pulsars

Anomalous X-ray Pulsars (AXPs; see Tables 1.1 and 1.2 for some characteristics) obtained their name because of their *anomalous* X-ray luminosity. The first member of this group that was discovered was 1E 2259+586 (Fahlman & Gregory 1981): a bright 6.98 s X-ray pulsar at the centre of a supernova remnant (G109.1-1.0; Fahlman & Gregory 1983). The 2–4 keV X-ray luminosity of $\sim 2 \times 10^{35}$ erg s^{-1} put the source in the luminosity range of X-ray binaries. However, neither significant orbital modulation could be detected from the X-ray data nor a bright optical counterpart could be identified and moreover, no radio counterpart was detected (Gregory & Fahlman 1983). A radio-pulsar like period derivative was derived to be 5×10^{-14} s s^{-1} (Koyama et al. 1987). The observed X-ray luminosity, however, was over three orders of magnitude higher than what could be explained by rotational energy loss (see Eq. 1.4).

Several additional sources were found with similar characteristics, though with larger period derivatives, and recognized as a different class of pulsars (Mereghetti & Stella 1995). Especially the narrow range of pulse periods (5.4 – 8.7 s) put them in a different regime than the high-mass X-ray binaries of which a wide range of pulse periods had been observed. Nevertheless, a low-mass X-ray binary scenario was more plausible than an interpretation as INSs (Mereghetti & Stella 1995). van Paradijs et al. (1995) proposed accretion from a circumstellar fossil disk to be the energy source.

The inferred magnetic fields from the periods and period derivatives and anomalously high X-ray luminosities made AXPs magnetar candidates. However, more observational evidence for magnetar behaviour, or observational disproof of another kind of origin was required to reach firm conclusions. AXPs turned out to be very stable rotators (against a binary inter-

pretation in which accretion plays a role) as phase-coherent timing was possible over time stretches of years for 1RXS J1708-40 and 1E 2259+586 (Kaspi et al. 1999).

In 2000 a first radio-pulsar-like glitch was detected from 1RXS J1708-40 (Kaspi et al. 2000). A larger glitch with a longer recovery time was detected 1.5 year later (Kaspi & Gavriil 2003; Dall'Osso et al. 2003). Glitching was predicted by the magnetar model, but other mechanisms could not be ruled out. Dall'Osso et al. (2003) explored different glitching theories and concluded that the starquake phenomenon in from the magnetar model was the most likely explanation. Only after the first AXPs exhibited bursting behaviour, the magnetar interpretation of AXPs seemed to become commonly accepted. 1E 1048.1-5937 was the first to show two bursts which were quite long compared to SGR-like bursts (Gavriil et al. 2002). Soon thereafter 1E 2259+586 showed over 80 SGR-like bursts (Kaspi et al. 2003; Gavriil et al. 2004) and the link between AXPs and SGRs was made. Both glitching and bursting behaviour have now been detected from several AXPs (Table1.1). As in SGRs, also large long-term torque variations are measured from AXP 1E 1048.1-5937 (Gavriil & Kaspi 2004).

Three AXPs have shown remarkably bright bursts ($\sim$2 orders of magnitude brighter than normal AXP bursts Woods et al. 2005). They all had SGR giant-flare-like characteristics, except for the absolute scale (e.g. the peak flux of the short initial spike and the integrated flux). They all showed a short bright peak and a long decaying tail lasting several hundred seconds in which (at the start of the tail) the pulsations of the pulsars were observed. In three bursts spectral emission features were observed (Gavriil et al. 2006, 2008a; Woods et al. 2005). Remarkably, all spectra have a spectral feature close to $\sim$13–14 keV in common. If these features would be due to proton cyclotron emission, then the surface magnetic field strengths of each pulsar would be $\sim(2-3)\times10^{15}$ G, which is high (but not too extreme) compared to the inferred magnetic-field strengths of these AXPs. Gavriil et al. (2008a) note that because these features are only observed in the brightest bursts it may be that these lines are atomic. This would open new opportunities to study the neutron-star crust and atmosphere.

The persistent X-ray spectra ($\sim$1–10 keV) of AXPs are all soft. A typical AXP spectrum can be canonically fitted with a black-body component with a temperature $kT\sim0.4-0.7$ keV plus a soft power-law component with photon index $\Gamma\sim3-4$. Naturally, the observed spectra are absorbed by interstellar material and therefore an absorption model has to be taken into account. More 'physical' models have been used to describe AXP spectra like double black-body models and photosphere modeling (e.g. Potekhin & Chabrier 2003; Lyutikov & Gavriil 2006; Güver et al. 2006; Fernández & Thompson 2007). So far no spectral features have been detected from persistent spectra. A claim was made by Rea et al. (2003), however this feature was not confirmed by other measurements (Rea et al. 2005).

AXPs can exhibit X-ray luminosity variability and periods of outbursts. During the bursting episode of 1E 2259+586, the source also showed a significant flux increase (2–10 keV) in total emission as well as in pulsed flux (Kaspi et al. 2003; Woods et al. 2004). Since then it has gradually decreased its persistent flux. 1E 1048.1-5937 shows occasional periods of increased pulsed flux which last a few months before returning to the normal level (Gavriil & Kaspi 2004; Gavriil et al. 2006). In 1998 the first transient AXP (candidate), AX J1845.0-

0258, was discovered in an archival ASCA observation from 1993 (Torii et al. 1998; Gotthelf & Vasisht 1998). In a second observation 3.5 years later it was an order of magnitude dimmer. More recent observations with *Chandra* yielded a possible counterpart which was at least 2 orders of magnitude dimmer than during its discovery (Tam et al. 2006). Unfortunately no pulsations were found and therefore no period derivative could be derived. The confirmation of AX J1845.0-0258 as AXP is pending a new outburst. In 2003 for the first time a firmly identified transient AXP was discovered. XTE J1810-197 was serendipitously discovered in outburst by Ibrahim et al. (2004) while observing SGR 1806-20. Archival ROSAT and ASCA data showed this source $\sim$2 orders of magnitude fainter than during discovery, just as AX J1845.0-0258.

Besides the outburst and some bursting activity XTE J1810-197 had another surprise (Woods et al. 2005). Halpern et al. (2005) reported a 9σ detection of this source in the radio band using VLA imaging observations. Soon thereafter Camilo et al. (2006) reported pulsed radio emission. They found XTE J1810-197 to be highly variable on the order of days and less. It shows an extraordinary power-law spectrum $S \propto \nu^{-0.5}$ (where ordinary radio pulsars have index $\sim$1.6). Moreover at frequencies higher than 20 GHz it is the brightest neutron star in the sky. The radiation is highly linearly polarized and also some circular polarization has been found by Kramer et al. (2007). The swings of the linear polarization in the position-angle–phase diagrams (i.e. the angle of the pulsar's magnetic field lines upon the plane of the sky; Radhakrishnan & Cooke 1969; Lyne & Manchester 1988) in the different observations are peculiar. They show long-term evolution which could suggest evolution in the magnetosphere. Moreover, the difference in angles between the main pulse and the interpulse is not 180°. If the pulses would be interpreted as two emission cones the magnetic poles are separated $\sim$190°. This can either be interpreted as an offset dipole or a higher order of field configuration (Kramer et al. 2007). The most recently confirmed AXP 1E 1547.0-5408 also showed pulsed radio emission (Camilo et al. 2007b, 2008). With a pulse period of 2.1 s it is the fastest rotating AXP known to date with a very high spin-down luminosity $\dot{E} = 1.0 \times 10^{35}$ erg s^{-1}.

With respect to the discovery of radio emission from magnetars, it needs to be noted that Malofeev et al. (2005) previously claimed radio emission from 1E 2259+586 at low radio frequencies. However, so far the observations/detections have not been confirmed with other telescopes.

The detection of AXPs in the optical and Near Infra Red (NIR) has proven to be very difficult as they are very dim (and absorbed). A breakthrough was made by Hulleman et al. (2000) with the first detection of 4U 0142+61 in the optical band ($R \sim 25$ mag). Together with I and V band measurements these proved to be much too dim for disk models. Hulleman et al. (2004) show that the colours are unusual. The flux points can not be explained by the Rayleigh-Jeans tail coming from the X-rays. They find a sudden drop in flux from the V to B band. Finally, they also show the first time variability in the NIR. A large fraction of the optical emission is pulsed (Kern & Martin 2002; Dhillon et al. 2005). This pulsed emission ruled out the possibility of an origin in a disk. A mid-infra-red excess has been discovered with *Spitzer* (Wang et al. 2006). It is interpreted as emission from a debris disk which is passive and therefore does not contribute to the X-ray luminosity.

The pulse profiles in $\sim$1–10 keV X-rays of AXPs can (more or less) be described by two components or a single sinusoidal-like pulse. The averaged pulsed fractions range from a few percent for 4U 0142+61 up to $\sim$60% for 1E 1048.1-5937. During outbursts the pulsed fraction can increase up to $\sim$94% (Tiengo et al. 2002). The pulse profiles of AXPs are in general very stable without significant or with very subtle pulse morphology changes over periods of years (Dib et al. 2007a, 2008a). After a bursting event or a glitch altered pulse shapes are observed. In the case of 1E 2259+586 the pulse morphology changed temporally while the source was in its active state. The 1E 2259+586 pulse profile recovered approximately to its former shape a few weeks after the bursting episode (Kaspi et al. 2003; Woods et al. 2004), contrary to the long-term profile change of SGR 1900+14. A change in magnetic-field configuration by crustal reconfiguration could explain the sudden pulse-shape change. This magnetic-field configuration apparently was just temporarily altered. Generally, pulse-shape morphology changes with energy are seen in most AXPs with a double peaked profile (see e.g. Sugizaki et al. 1997; Israel et al. 2001; Kuiper et al. 2006).

So far, only from 4U 0142+61 pulsed optical emission has been observed (Kern & Martin 2002; Dhillon et al. 2005). The pulse profile is broad and maybe double peaked as in the X-ray band. The quality of the optical pulse profile is not sufficient to conclude whether the optical profile coaligns with one, both or none of the X-ray pulses. Compared with pulse profiles below 1 keV they seem not to align in phase. If the X-rays in this energy band are mainly thermal one might not expect a phase alignment (Kern & Martin 2002). Compared with the integrated 2–10 keV pulse profile the optical profile might align with the dominating pulse, or maybe even with both (Dhillon et al. 2005). If both profiles are dominated by non-thermal emission (caused by the same physical mechanism, and at the same site) a phase alignment is expected.

The radio pulse profiles in the radio are very different from all other pulse shapes. The pulse profiles from XTE J1810-197 are very narrow and spiky (Camilo et al. 2007d) while the X-ray pulse profile is almost sinusoidal. However, the maxima of the radio and X-ray peaks almost align. The pulse profiles are very variable as a function of time (Camilo et al. 2007a,d). Contrary to radio pulsars no stable pulse profile is generated after adding a large number of single pulses (Kramer et al. 2007). Also the radio pulse profiles show significant morphology changes as a function of energy, and show a large degree of linear polarization (Camilo et al. 2006, 2007c).

1.5.4 Hard Anomalous X-ray Pulsars

The discussion whether AXPs and SGRs are magnetars has settled down. Most/all observed quantities can be explained within the magnetar model. However, in 2004 hard X-rays ($>$20 keV) were detected with INTEGRAL from the directions of 2 AXPs (1E 1841-045 and 1RXS J1708-40; Molkov et al. 2004; Revnivtsev et al. 2004a). Soon thereafter den Hartog et al. (2004a) discovered hard X-rays from the location of a third AXP, 4U 0142+61.

The first for which it was shown that the hard X-ray emission indeed originated from the magnetar was 1E 1841-045. Because 1E 1841-045 is situated within supernova remnant

Kes 73 (G27.4+0.0; Sanbonmatsu & Helfand 1992), the supernova remnant could in principle be responsible for the hard X-ray emission. However, for a supernova remnant it would have been very bright and the spectrum very hard. With a timing analysis of the first four years of archival RXTE data Kuiper et al. (2004a) showed that the signal from 1E 1841-045 had a significant pulsed component in the hard X-ray band. It proved unambiguously that the AXP was indeed the hard X-ray emitter. This was completely unexpected, given the very soft spectra known below 10 keV for all AXPs.

Using both RXTE-PCA and HEXTE a total-pulsed spectrum was extracted from the data up to $\sim$150 keV. The spectrum above 10 keV could be described with a power law with photon index $\Gamma = 0.94 \pm 0.16$. This is significantly harder than the estimated total-spectrum using HEXTE which showed a power-law with photon index $\Gamma = 1.47 \pm 0.05$[1], meaning the pulsed fraction is increasing with energy. Above $\sim$10 keV the spectrum of 1E 1841-045 shows now an upturn. Around this energy the AXP changes its soft character into a very hard one. Moreover, the luminosity above 10 keV is even higher than below 10 keV.

With this discovery by Kuiper et al. (2004a) a new era in magnetar astrophysics started. Luminous persistent non-thermal hard X-ray emission was **not** predicted by the magnetar model.

Hard non-thermal emission was so far only considered as a transient phenomenon during magnetar bursts (Thompson et al. 2002). Starting from the twisted-magnetosphere model (Thompson et al. 2002), Thompson & Beloborodov (2005) presented the first concept for an extension to the magnetar model with processes which could be capable of producing sufficient and hard non-thermal emission. This concept would evolve into the so-called magnetar *corona* model (Beloborodov & Thompson 2007).

Thompson & Beloborodov (2005) propose two possible mechanisms which are capable of producing stable hard X-ray emission. The first mechanism is surface emission. A thin surface layer can be heated by a downward beam of charged particles up to $kT \sim 100$ keV. The expected spectrum is bremsstrahlung-like and is slightly modified by Compton heating. The second mechanism is magnetospheric emission at $\sim$100 km above the neutron-star surface. A synchrotron spectrum is expected to originate from pairs which are created from accelerated positrons which Compton scatter keV photons.

These mechanisms are capable of producing spectra which are consistent with the observed total spectrum of 1E 1841-045 by Kuiper et al. (2004a). Even though pulsed emission is possible for these mechanisms it is hard to explain the increasing pulsed fraction as a function of energy.

This was the scientific status (observationally and theoretically) at the time when the study of AXPs for this thesis started.

Besides the cited papers the following sources were used for this introduction: Shapiro & Teukolsky (1983), Kippenhahn & Weigert (1990), Jackson (1998), Lorimer & Kramer (2004), Woods & Thompson (2006) and Harding (2008).

[1] Note this HEXTE spectrum is contaminated by the diffuse Galactic X-ray background, an improved INTEGRAL spectrum is presented by Kuiper et al. (2006) in Chapter 4.

1.6 Contents of this thesis

Chapter 3: A wide-field spectral-imaging study with INTEGRAL – In this chapter we analyse a deep INTEGRAL (20–200 keV) exposure of a large region in the sky including Cassiopeia. We exploit the very good imaging capabilities of the imager IBIS onboard INTEGRAL. A spectral study is performed on the detected sources. These sources include several X-ray binaries, of which two are new hard X-ray sources. The most surprising result in this work is the discovery of hard X-rays from AXP 4U 0142+61. The hard X-ray emission is detected up to $\sim$150 keV with a power-law like spectrum with index $\Gamma = 0.73 \pm 0.17$. Compared to the very soft X-ray spectrum ($\Gamma \sim 3.6$) below 10 keV, this means an unexpected drastic upturn of the spectrum. AXPs have become hard X-ray sources. Moreover, we show that the bulk of the energy emitted by this AXP is emitted above 10 keV. Its 20–100 keV luminosity is 5.9×10^{34} erg s^{-1}(assuming a distance of 3 kpc), which is more than two orders of magnitude more luminous than its maximum spin-down luminosity (see Eq. 1.4). We revisited COMPTEL (0.75–3 MeV) archival data and derived only flux upper limits. The implication is that the hard X-ray spectrum has to break between $\sim$75 keV and $\sim$750 keV.

Chapter 4: Pulsed hard X-ray emission from AXPs – Kuiper et al. (2004a) showed for the first time that an AXP (1E 1841-045) produces pulsed hard X-ray emission ($>$10 keV). In this chapter we show the discovery of pulsed hard X-ray emission from three more AXPs using archival RXTE data. Very hard X-ray total and total-pulsed spectra are found for AXPs 4U 0142+61 and 1RXS J1708-40 using RXTE and INTEGRAL data. For 1E 2259+586 only a hardening of the pulsed spectrum is detected between 10 keV and 24 keV. This AXP is too weak to detect a possible hard X-ray spectral component with a similar shape as discovered for the other three AXPs. Also for these AXPs no signal was found in archival COMPTEL data. The pulse profiles of these sources have been studied. Their shapes gradually change as a function of energy.

Chapter 5: A multi-wavelength study of 4U 0142+61 – As will become clear in this thesis, studying an AXP in a broad spectral domain leads to more insights than narrow-band studies. The bulk of the energy is emitted in X-rays ($\sim$0.5–10 keV) and in hard X-rays ($\sim$10–250 keV), but important clues on non-thermal emission mechanisms could be found in the radio and optical/NIR regimes. In this section we present the results of a (quasi) simultaneous multi-wavelength study of 4U 0142+61. During a dedicated 1 Ms INTEGRAL observation we also performed observations in the X-ray domain with *Swift*, optical/NIR observations with *Gemini* and radio observations with WSRT. The same hard X-ray spectrum as reported in the previous chapters was found in the INTEGRAL domain, confirming its persistent nature. This time we measured a power-law like spectrum with photon index $\Gamma = 0.79 \pm 0.10$ which was detected up to 230 keV thanks to the higher exposure. No indication for a spectral break was found up to this high energy. The optical and NIR flux measurements are up to two to three orders of magnitude higher than what one would expect by extrapolating the INTEGRAL and *Swift* spectra. This remains unexplained. Unfortunately, no radio detection was achieved in a 12-hour observation with the WSRT.

Chapter 6: Detailed high-energy characteristics of 4U 0142+61 – To derive constraints for modelling the physical processes responsible for the production of the non-thermal emission from AXPs, detailed observational characteristics are needed for the whole high-energy window. To derive these characteristics we used all 4.5 Ms INTEGRAL data taken over three years, three sets of XMM-*Newton* data, a set of ASCA-GIS data and 7.5 years of RXTE-monitoring data. This extensive study yielded in the INTEGRAL band a time-averaged power-law like total spectrum with photon index $\Gamma = 0.93 \pm 0.06$, detected up to 230 keV. A significant deviation from this power-law spectrum is measured thanks to constraining INTEGRAL-SPI limits above 230 keV. The maximum luminosity of 4U 0142+61 is estimated to be around 280 keV. No time variability in the INTEGRAL domain was found. The source is stable within the 17% level (1σ) both in spectral shape and in flux. A timing study has been performed on all INTEGRAL data and pulsed emission of 4U 0142+61 has been detected up to 160 keV. The pulsed spectrum is very hard and can be described with a power-law with photon index $\Gamma = 0.40 \pm 0.15$. Timing analyses were also performed on the XMM-*Newton*, RXTE and ASCA-GIS data. We found that the pulse profiles taken with ASCA-GIS are significantly different from the XMM-*Newton* observations which seems to be due to a possible glitch. Using these timing analyses, we performed broad-band phase-resolved spectroscopy over the total 0.8–300 keV high-energy band . We extracted for three broad phase intervals the pulsed spectra. These exhibited vastly different spectra over the total high-energy band. Our main conclusion is that at least three genuinely different pulse components with different spectra are identified. The consistent results from the four missions with observations at different epochs indicate a remarkable stable overall geometry in the magnetosphere of this AXP. We discussed these results with respect to models proposed to explain the non-thermal hard X-ray emission.

Chapter 7: The bizarre AXP 1RXS J1708-40 – For this AXP the same approach as for 4U 0142+61 in Chapter 6 was chosen to verify whether also for this AXP genuinely different spectral components can be identified. Again, using all available INTEGRAL data, 12 Ms this time, one XMM-*Newton* observation, and all available RXTE data spanning nine years. As for 4U 0142+61 we find for 1RXS J1708-40 also a stable INTEGRAL total-spectrum over the time span of four years. The time-averaged INTEGRAL spectrum is power-law like with a photon index $\Gamma = 1.13 \pm 0.06$ reaching up to $\sim$175 keV. No constraining SPI limits were obtained and therefore no spectral break could be identified. Surprisingly, the pulse profile and pulsed emission could be measured up to 270 keV. The INTEGRAL total-pulsed spectrum could be described by a power law with index $\Gamma = 0.98 \pm 0.31$. The phase-resolved spectra from this source appear to show spectacular variations in shape. First we used three broad phase intervals for all INTEGRAL, RXTE and XMM-*Newton* data. The spectra accumulated by the different missions at different epochs are overlapping in energy and the transitions from one instrument to another are smooth. Also for this AXP this is indicative for an overall stable geometry over the time span of years. The three phase-resolved spectra do not follow the shape of the total-pulsed spectrum and are significantly more complex. Motivated by these broad phase-interval spectra we performed phase-resolved spectroscopy for 10 narrow phase bins for INTEGRAL and RXTE. This lead to the identification of three different spectral

components: a soft power law with index $\Gamma = 3.58 \pm 0.34$, a hard power law with index $\Gamma = 1.00 \pm 0.09$ and a curved component modelled with two logparabolic functions. They can explain the pulsed spectra as a function of phase and represent decoupled pulse profiles which together constitute the total pulse profile. A complete decoupling has been achieved of the high-energy emission from 1RXS J1708-40 based on the detailed spectral and temporal characteristics, providing tide constraints on the interpretation.

1.7 Summary

Anomalous X-ray Pulsars (AXPs) were traditionally spectrally soft X-ray sources ($<$10 keV). Soon after the launch of INTEGRAL, AXPs were discovered in the hard X-ray domain ($\sim$20–300 keV). Around 10 keV the spectra of some AXPs were shown to switch from spectrally soft ($\Gamma \sim 3-4$) to hard ($\Gamma \sim 1$). This transition is not only surprising, but there is also no agreed explanation. In this thesis we perform observational studies for several AXPs and study both the soft and the hard X-ray characteristics. This is done by using (almost) all available data from different X-ray/gamma-ray observatories. Spectral and temporal analyses are presented. Spectral details from the total spectra, total-pulsed spectra and also from phase-resolved spectra are shown and discussed. Pulse-profile comparisons and pulse profiles as a function of energy are presented and discussed. Important clues are found for the magnetospheric stability of AXPs. The typically spectrally soft 'character' of AXPs has completely changed to a hard one over the last few years. In this thesis we present the results which made this happen. The detailed characteristics provide stringent constraints for future AXP modeling which should ultimately lead towards the full understanding of the extreme physical processes occurring under the extreme conditions in the magnetospheres of AXPs.